

# RSC Advances



This is an *Accepted Manuscript*, which has been through the Royal Society of Chemistry peer review process and has been accepted for publication.

*Accepted Manuscripts* are published online shortly after acceptance, before technical editing, formatting and proof reading. Using this free service, authors can make their results available to the community, in citable form, before we publish the edited article. This *Accepted Manuscript* will be replaced by the edited, formatted and paginated article as soon as this is available.

You can find more information about *Accepted Manuscripts* in the [Information for Authors](#).

Please note that technical editing may introduce minor changes to the text and/or graphics, which may alter content. The journal's standard [Terms & Conditions](#) and the [Ethical guidelines](#) still apply. In no event shall the Royal Society of Chemistry be held responsible for any errors or omissions in this *Accepted Manuscript* or any consequences arising from the use of any information it contains.



Journal Name

ARTICLE

## A colorimetric and ratiometric fluorescence probe for detection of palladium in the red light region

Kaiqiang Xiang,<sup>a</sup> Yunchang Liu,<sup>a</sup> Changjiang Li,<sup>a</sup> Baozhu Tian\*<sup>a</sup> and Jinlong Zhang\*<sup>a</sup>

Received 00th January 20xx,  
Accepted 00th January 20xx

DOI: 10.1039/x0xx00000x

www.rsc.org/

Developing probes for selective and sensitive detection of palladium in living organisms is of great importance. In this work, we synthesized a colorimetric and ratiometric fluorescence probe (Probe 1) with red light emission ( $\lambda_{em} = 643$  nm) by employing isophorone based fluorescent dye as fluorophore and allylcarbamate group as response unit. Based on the Pd<sup>0</sup>-triggered cleavage reaction, Probe 1 showed high response speed, selectivity, and sensitivity towards palladium species. Upon addition of palladium, the absorption and emission spectra of Probe 1 exhibited obvious red-shift, which can be easily discriminated by naked eyes. In terms of palladium, the detection limit is as low as 24.2 nM and the signal-to-noise ratio in fluorescence intensity can reach 85-fold. As a red emitting ratiometric sensor, Probe 1 can be potentially used for quantitative detection of palladium in living organisms.

### Introduction

Palladium, a rare inner transition metal, is widely used in various materials such as dental crowns, catalytic converters, fuel cells, and jewellery as precious metal.<sup>1–3</sup> Despite the importance of palladium in such applications, subsequent damage to organisms with its frequent use (synthetic, medicinal and bioorthogonal organometallic chemistry) is a major downfall.<sup>4</sup> It can bind to DNA, protein, and other biomolecules, which disturbs biological processes.<sup>5–7</sup> Intracellular palladium is emerging as an exogenous metal that is of interest in recent years for those involved in BOOM chemistry (to unmask bioactive compounds upon the addition of palladium) and drug delivery.<sup>8</sup> Therefore, it is significant to develop some selective and sensitive methods for detection of palladium and its derivatives.<sup>9</sup> Several typical analytical methods, such as atomic absorption spectroscopy (AAS), inductively coupled plasma mass spectrometry (ICP-MS), solid phase micro extraction-high performance liquid chromatography and X-ray fluorescence, have been used for the quantitative detection of palladium species.<sup>10,11</sup>

Among different analytical methods available, fluorescent imaging is considered to be the most sensitive approach because of its sensitivity and simplicity.<sup>12</sup> According to the recent reports, colorimetric and ratiometric fluorescent probes have many advantages such as the convenience and aesthetic appeal.<sup>13–18</sup> Particularly, ratiometric measurements have the important feature of permitting signal rationing, which can

increase the dynamic range and provide built-in correction for environmental effects.<sup>19,20</sup> However, most of the palladium probes via fluorescence turn-on response have two main shortages: one is the single detection window, which always influences its quantitative detection because of environmental effects; the other is the short excitation wavelength, which limits their application in vivo.<sup>21–26</sup> Therefore, it is of significant importance to develop some ratiometric palladium probes that can emit in the red or NIR light region, because the longer wavelength fluorescence would not be disturbed by the auto-fluorescence taking place in indigenous biomolecules of the living systems.<sup>27,28</sup>

Isophorone based fluorescent dyes are well known for its excellent properties in Dye-sensitized solar cells and organic nonlinear optical crystals.<sup>29–32</sup> These dyes basically have typical donor- $\pi$ -acceptor (D- $\pi$ -A) structure, longer emission wavelength in the red (or NIR) region, and large Stokes shift from the ultrafast intramolecular charge transfer (ICT).<sup>33</sup> However, to the best of our knowledge, isophorone based fluorescent dyes have not been employed in fluorescence sensors. Herein, we designed a novel colorimetric and ratiometric palladium sensor (Probe 1) emitting in the red region (Scheme 1) by employing isophorone based fluorescent dye as the fluorophore and allylcarbamate group as the response unit. After reaction with palladium, the allylcarbamate group can cleave the carbamate linkage and release the amino group.<sup>34</sup> The probe can meet the criteria of both emitting in the red wavelength region and quantitative visual detection. At the same time, it showed high sensitivity and selectivity toward palladium.

### Experimental

#### Synthesis of compound 3<sup>35</sup>

<sup>a</sup> Key Lab for Advanced Materials and Institute of Fine Chemicals, East China University of Science and Technology, 130 Meilong Road, Shanghai 200237, PR China. E-mail: baozhutian@ecust.edu.cn; jlzhang@ecust.edu.cn. Electronic Supplementary Information (ESI) available: [details of any supplementary information available should be included here]. See DOI: 10.1039/x0xx00000x

Isophorone (5.0 g, 36.2 mmol) was dissolved in absolute EtOH (50.0 mL), followed by addition of malononitrile (2.87 g, 43.4 mmol) and piperidine (0.5 g, 4.8 mmol). Then, the mixture was refluxed for 12 h under N<sub>2</sub> atmosphere. After the solvent being removed, the precipitation was dissolved in CH<sub>2</sub>Cl<sub>2</sub>, washed with water, and dried over Na<sub>2</sub>SO<sub>4</sub>. Finally, the solvent was evaporated in vacuum, and the raw product was purified by silica column chromatography under Petroleum/Ethyl acetate = 5:1(v/v) to give a white solid (4.72g, 70%). <sup>1</sup>H-NMR (400 MHz, CDCl<sub>3</sub>): δ = 6.61(s, 1H), 2.51 (s, 2H), 2.19 (s, 2H), 2.04 (s, 3H), 1.01 (s, 6H) (Fig. S1). <sup>13</sup>C-NMR (100 MHz, CDCl<sub>3</sub>): δ = 170.51, 160.06, 120.50, 113.22, 112.44, 78.04, 45.60, 42.61, 32.36, 27.79, 25.32 (Fig. S2).

### Synthesis of Compound 2<sup>36</sup>

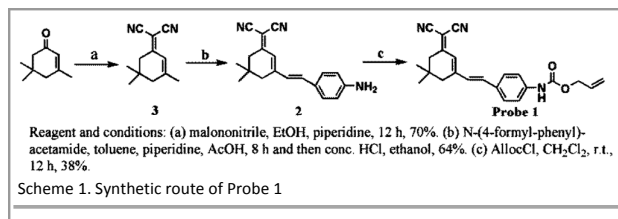
Under nitrogen atmosphere, compound 3 (300 mg, 1.6 mmol) and N-(4-formyl-phenyl) acetamide (263 mg, 1.6 mmol) were added to toluene (20 mL) containing piperidine (0.3 mL) and acetic acid (0.3 mL). Subsequently, the above mixture solution was refluxed for 8 h to give an orange precipitate. After filtration, the orange solid was refluxed in a mixed solution of concentrated HCl (20 mL) and ethanol (10 mL) for another 16 h. Then, the pH of the solution was adjusted to neutral and it was extracted with ethyl acetate. Finally, the organic layers were dried over Na<sub>2</sub>SO<sub>4</sub>, filtered, and concentrated to obtain the crude product, which was purified by silica column chromatography using CH<sub>2</sub>Cl<sub>2</sub> as an eluent to yield Compound 2 (crimson solid, 340 mg, 64%). <sup>1</sup>H-NMR (400 MHz, CDCl<sub>3</sub>): δ = 7.41 (d, J = 8 Hz, 2H), 7.10 (m, 2H), 6.70 (s, 1H), 6.57 (d, J = 8 Hz, 2H), 5.87 (s, 2H), 2.55 (s, 2H), 2.49 (s, 2H), 1.00 (s, 6H) (Fig. S3). <sup>13</sup>C-NMR (100 MHz, DMSO): δ = 169.80, 157.46, 151.34, 139.75, 130.12, 123.35, 119.94, 114.53, 113.76, 113.71, 72.69, 42.98, 39.69, 31.58, 27.43 (Fig. S4). HRMS (ESI): calcd. for [C<sub>19</sub>H<sub>19</sub>N<sub>3</sub> + H]<sup>+</sup> 290.1657; found 290.1657 (Fig. S5).

### Synthesis of Probe 1

At 0 °C, a mixture of AllocCl (1.0 mL) and CH<sub>2</sub>Cl<sub>2</sub> (5 mL) was added dropwise to a solution of CH<sub>2</sub>Cl<sub>2</sub> solution (15 mL), Compound 2 (200 mg, 0.69 mmol), and triethylamine (0.5 mL). After being stirred for 30 min, the mixture was heated to room temperature and stirred overnight. Then, the mixture was concentrated under vacuum and the crude product was purified by silica column chromatography under Petroleum/CH<sub>2</sub>Cl<sub>2</sub> = 1:1 (v/v) to give a yellow solid (98 mg, yield: 38%). <sup>1</sup>H-NMR (400 MHz, CDCl<sub>3</sub>): δ = 9.99 (s, 1H), 7.64 (d, J = 8 Hz, 2H), 7.51 (d, J = 8 Hz, 2H), 7.25 (m, 2H), 6.82 (s, 1H), 6.00 (m, 1H), 5.37 (dd, J = 4 Hz, J = 8 Hz, 1H), 5.25 (dd, J = 4 Hz, J = 8 Hz, 1H), 4.63 (d, J = 8 Hz, 2H), 2.59(s, 2H), 2.52 (s, 2H), 1.01 (s, 6H) (Fig. S6). <sup>13</sup>C-NMR (100 MHz, CDCl<sub>3</sub>): δ = 170.21, 156.19, 152.98, 140.53, 137.49, 130.11, 122.02, 117.72, 113.96, 113.16, 75.70, 64.81, 39.68, 38.10, 31.62, 27.39 (Fig. S7). HRMS (ESI): calcd. For [C<sub>23</sub>H<sub>23</sub>O<sub>2</sub>N<sub>3</sub>-H]<sup>+</sup> 372.1712; found 372.1710 (Fig. S8).

### Characterization and Detection

<sup>1</sup>H NMR and <sup>13</sup>C NMR spectra were recorded on Bruker AM-400 MHz instruments with TMS as internal standard. HRMS was performed on Waters LCT Premier XE spectrometer. UV–



Vis absorption spectra of the samples were conducted on a SHIMADZU UV–Vis spectrophotometer. The fluorescence spectra were measured with a SHIMADZU RF-5301PC fluorescence spectrophotometer by using 472 nm line of Xe lamp as excitation source at room temperature.

The detection limit of Probe 1 was calculated according to the previous report.<sup>37–40</sup> The fluorescence emission spectrum of Probe 1 was measured by five times to achieve the standard deviation ( $\sigma$ ) of blank measurement.<sup>21</sup> In order to obtain the slope (S), the ratio of the fluorescence intensity at 570 nm and 643 nm were plotted as a function of palladium concentration (0–1  $\mu$ M). The detection limit was calculated with the following formula:  $3\sigma/S$ .

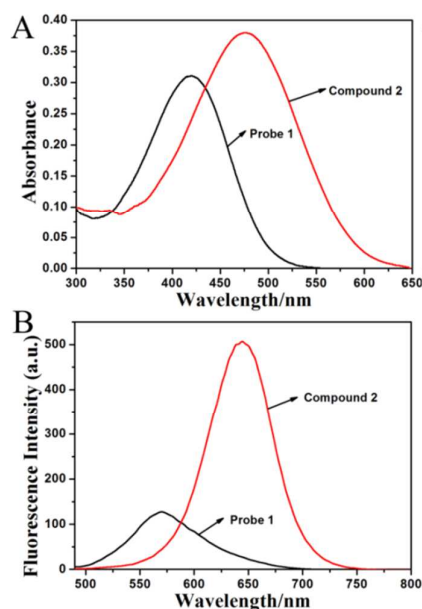
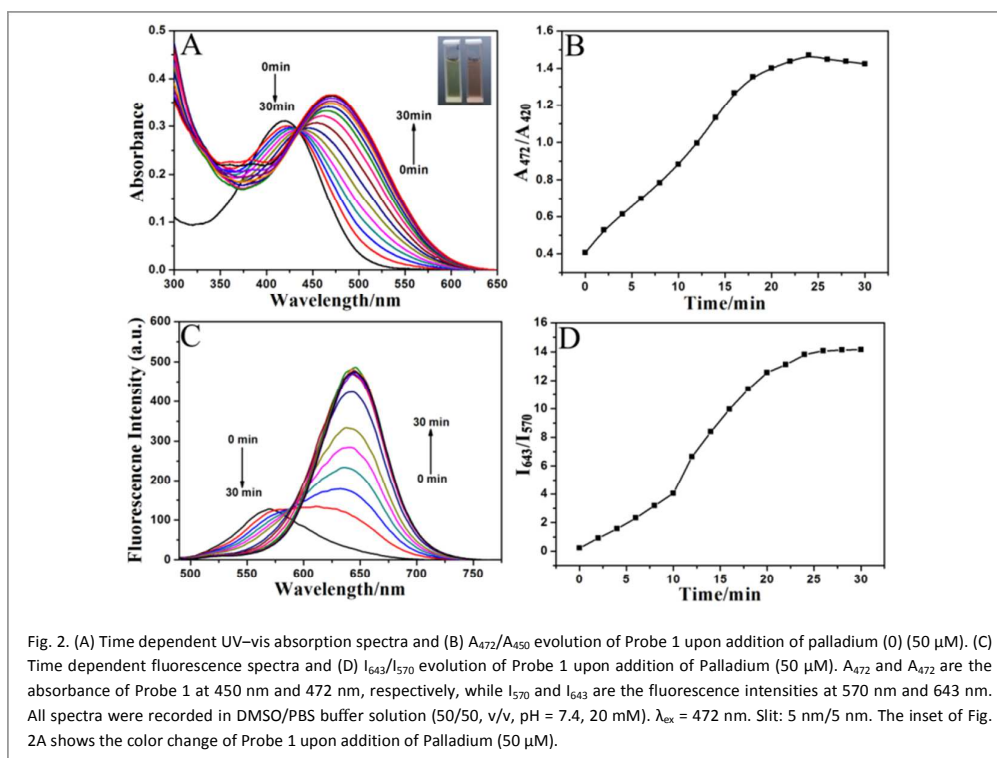


Fig. 1. (A) UV–vis absorption and (B) Fluorescence spectra of Probe 1 and Compound 2. All spectra were recorded in DMSO/PBS buffer solution (50/50, v/v, pH = 7.4, 20 mM).  $\lambda_{\text{ex}}$  = 472 nm. Slit: 5 nm/5 nm.

## Result and discussion

### Synthesis route

The synthetic route of Probe 1 is illustrated in scheme 1. Firstly, compound 3 was synthesized by the reaction of isophorone and malonitrile in EtOH. Then, compound 3 reacted with N-(4-formyl-phenyl)acetamide in presence of acetic acid and piperidine, followed by treatment with concentrated HCl to generate Compound 2 in EtOH. Finally, Probe 1 was obtained by the reaction of Compound 2 and AllocCl in DCM at room temperature.<sup>28</sup> Structural identification of Probe 1, compound 3,



and Compound 2 was confirmed by NMR and HRMS spectroscopy (Fig. S1–Fig. S8).

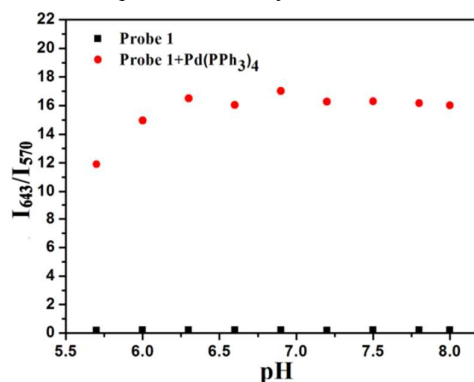
#### Properties of Probe 1

Fig. 1 shows the UV–vis absorption and fluorescence spectra of Probe 1 and Compound 2. As shown in Fig. 1A and 1B, Probe 1 exhibits a typical ICT broad absorption peak at 420 nm (Fig. 1A) and weak fluorescence emission peak at 570 nm (Fig. 1B), while Compound 2 presents a red-shifted absorption peak at 472 nm and a strong fluorescence at 643 nm. The fluorescence quantum yields of Probe 1 and Compound 2 were determined to be 0.003 and 0.016, respectively, by using Rh 6G ( $\Phi = 0.94$ , in EtOH) as reference (Table S1). Both Probe 1 and Compound 2 show large Stokes shifts (150 nm for Probe 1 and 170 nm for Compound 2), which is relative to the D- $\pi$ -A structures of Probe 1 and Compound 2. The distinct difference between Compound 2 and Probe 1 in the spectroscopic properties can be explained as follows: For Compound 2, due to the strong electron donating ability of amino group, the donor- $\pi$ -acceptor (D- $\pi$ -A) structure shows high dipole moment, resulting in evident red-shifts of absorption and emission spectra. In the case of Probe 1, the electron donating ability of the nitrogen atom was deprived by the electron-withdrawing carbonyl group,<sup>28</sup> thus the dipole moment of donor- $\pi$ -acceptor (D- $\pi$ -A) structure would dramatically decline. As a result, the absorption and emission peaks would shift to shorter wavelength.

To investigate the reaction property of Probe 1, initial spectroscopic studies were conducted by monitoring the changes of the absorption and fluorescence spectra upon addition of Pd(PPh<sub>3</sub>)<sub>4</sub> in DMSO/PBS buffer solution (50/50, v/v, pH = 7.4, 20 mM). As shown in Fig. 2A and 2B, after

adding palladium (50  $\mu$ M) to Probe 1, the absorption at 472 nm increases gradually, along with the depression of absorption at 420 nm ( $\Delta\lambda_{\text{abs}} = 52$  nm), corresponding to a color change from yellow to pink (the inset of Fig. 2A). Meanwhile, the emission band at 570 nm decreases gradually and a new band at 643 nm emerges ( $\Delta\lambda_{\text{em}} = 73$  nm). With a palladium concentration of 50  $\mu$ M, the ratio of fluorescence intensities at 643 nm and 570 nm ( $I_{643}/I_{570}$ ) reaches 85 (Fig. 2C and 2D), revealing that Probe 1 has a high signal-to-noise ratio. It is worth noting that the observed fluorescence intensity increased after Probe 1 was totally transformed to Compound 2. The reason can be explained as follows: Possessing two electron-withdrawing groups (EWG), dicyano group and carbonyl moiety, Probe 1 as a “pull-pull” system blocks the ICT process. After addition of Pd, the amide moiety will be converted into amino moiety. As an electron-donating group (EDG), the amino moiety can increase the fluorescence intensity by forming a “push-pull” system.<sup>41–44</sup>

Additionally, both absorption and emission spectra reach a plateau within 30 min (Fig. 2B, D), indicating that the response rate of Probe 1 to palladium is very fast.



**Fig. 3.** Effect of pH on  $I_{643}/I_{570}$  of Probe 1 (10  $\mu\text{M}$ ) in DMSO/ $\text{NaH}_2\text{PO}_4$ - $\text{Na}_2\text{HPO}_4$  solution (1/1, v/v).  $\lambda_{\text{ex}} = 472 \text{ nm}$ . Slit: 5 nm/5nm.

### Effect of pH

To explore the applicability of Probe 1 in real biological systems, the effect of pH on the fluorescence response of Probe 1 to palladium was evaluated in the pH range of 5.7–8.0. As shown in Fig. 3,  $I_{643}/I_{570}$  shows a slight increase in the pH range of 5.7–6.2 and almost keeps unchanged in the pH range of 6.2–8.0. This result indicates that Probe 1 is stable in biological systems and can be employed as a capable candidate for palladium detection.

### Sensitivity

The recognition ability of Probe 1 to palladium in DMSO/PBS buffer solution (50/50, v/v, pH = 7.4, 20 mM) was also investigated by the UV-vis absorption and fluorescence titration experiments. As shown in Fig. 4A, The absorption at 420 nm decreases gradually with increasing the concentration of  $\text{Pd}(\text{PPh}_3)_4$  from 0 to 20  $\mu\text{M}$ , together with the enhancement of absorption at 472 nm. The absorbance ratio at 472 nm and 420 nm ( $A_{472}/A_{420}$ ) has a good linearity ( $R = 0.9957$ ) as a function of palladium concentration (0–20  $\mu\text{M}$ ) (Fig. 4B). Similarly, the intensity of fluorescence emission at 570 nm decreases gradually, along with the evident increase of fluorescence emission at 643 nm (Fig. 4C). Fig. S9 shows the

plot of fluorescence intensity ratio at 643 nm and 570 nm as a function of palladium concentration. Obviously, the plot fits linearly with a correlation coefficient of 0.9694 in the palladium concentration range of 0–1  $\mu\text{M}$ . The detection limit of Probe 1 was estimated to be as low as 24.2 nM. This result indicated that Probe 1 is quite suitable to quantitatively detect low concentration of palladium, similar to the previous reports (Table S2).

### Reaction mechanism

The excellent selectivity should be attributed to the highly specific Pd0-triggered cleavage process.<sup>23,45</sup> A feasible fluorescence sensing mechanism is shown in Scheme 2. Firstly, as a trigger moiety, allylcarbamate conjugates with palladium and ionizes to form Probe 1-Pd. Next, carbamate 2 is formed by dissociation. Finally, carbamate 2 transforms into Compound 2 by decarboxylation. Because Probe 1 and Compound 2 have different absorption and emission wavelengths, the presence/or absence of Pd can be easily identified. Moreover, the conversion rate of probe 1 is positively relative to Pd content, so, we can estimate the Pd concentration in solution by analyzing the variation of fluorescence intensities at 570 nm and 643 nm. To confirm this mechanism, the product after the reaction between Probe 1 and palladium was isolated and checked via TLC. The result showed that the reaction product is Compound 2 (Fig. S10), which was further proved by the peak at 290.1653 in the HRMS (theoretical mass: 290.1657) (Fig.

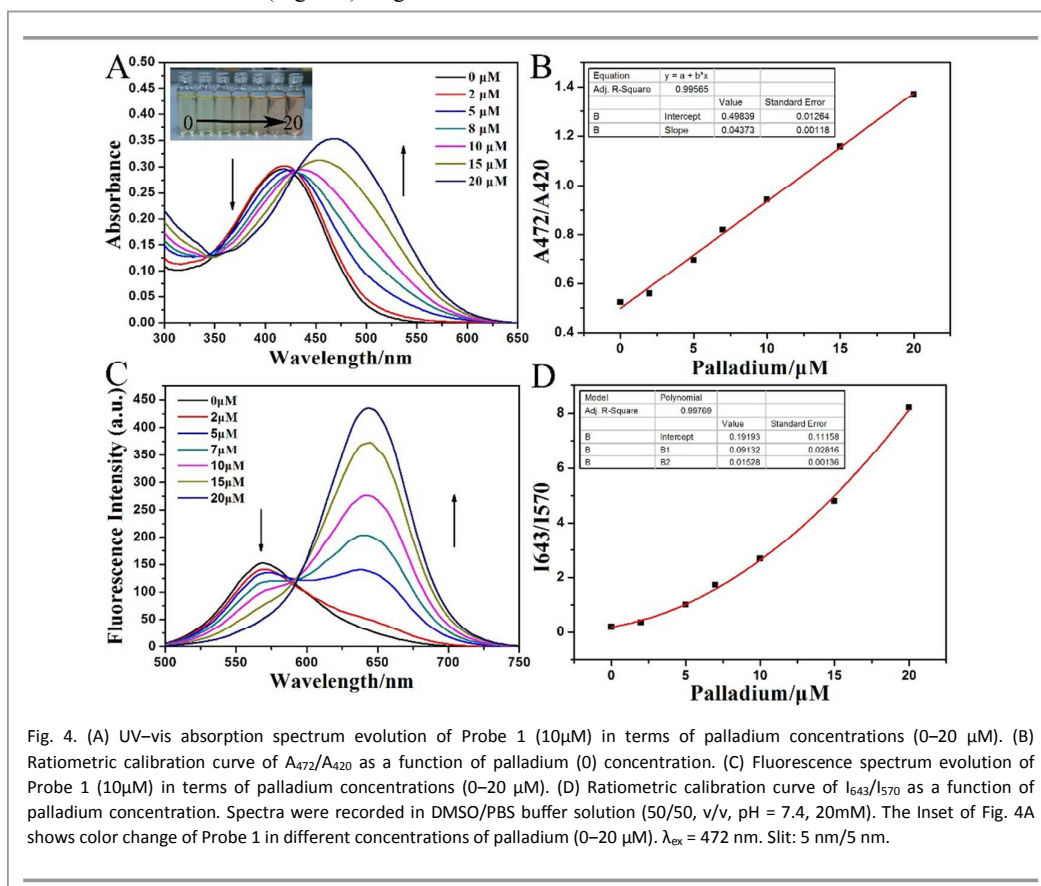
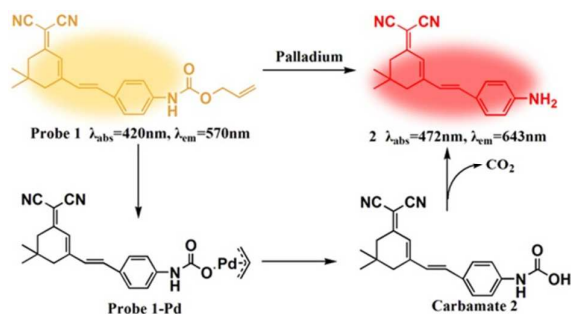


**Fig. 4.** (A) UV-vis absorption spectrum evolution of Probe 1 (10  $\mu\text{M}$ ) in terms of palladium concentrations (0–20  $\mu\text{M}$ ). (B) Ratiometric calibration curve of  $A_{472}/A_{420}$  as a function of palladium (0) concentration. (C) Fluorescence spectrum evolution of Probe 1 (10  $\mu\text{M}$ ) in terms of palladium concentrations (0–20  $\mu\text{M}$ ). (D) Ratiometric calibration curve of  $I_{643}/I_{570}$  as a function of palladium concentration. Spectra were recorded in DMSO/PBS buffer solution (50/50, v/v, pH = 7.4, 20mM). The inset of Fig. 4A shows color change of Probe 1 in different concentrations of palladium (0–20  $\mu\text{M}$ ).  $\lambda_{\text{ex}} = 472 \text{ nm}$ . Slit: 5 nm/5 nm.

S11). Moreover, the changes of both UV-vis absorption and fluorescence spectra upon addition of palladium further confirmed the above-mentioned reaction mechanism (Fig. S12).



Scheme 2. Mechanism for selective recognition of palladium (0).

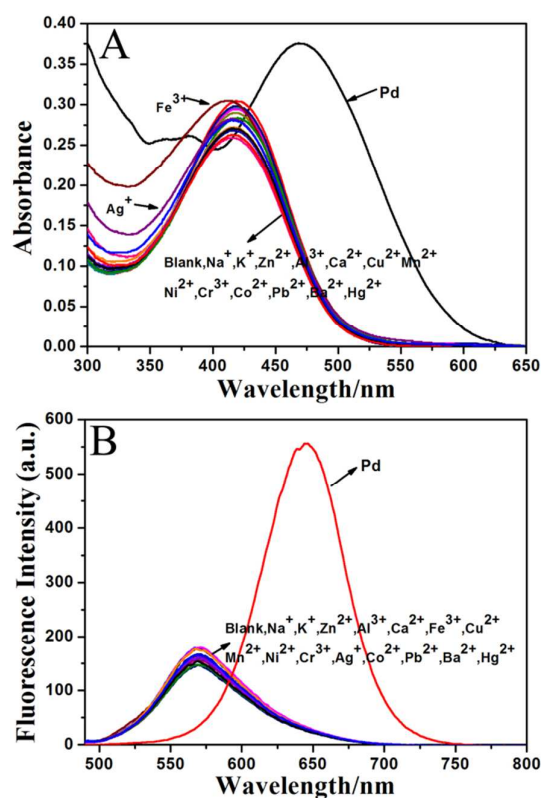


Fig. 5. (A) UV-vis absorption and (B) fluorescence spectra of Probe 1 upon addition of various metal ions: Na<sup>+</sup>, K<sup>+</sup>, Zn<sup>2+</sup>, Al<sup>3+</sup>, Ca<sup>2+</sup>, Fe<sup>3+</sup>, Cu<sup>2+</sup>, Mn<sup>2+</sup>, Ni<sup>2+</sup>, Cr<sup>3+</sup>, Ag<sup>+</sup>, Co<sup>2+</sup>, Pb<sup>2+</sup>, Ba<sup>2+</sup> and Hg<sup>2+</sup> (50 μM). All spectra were recorded in DMSO/PBS buffer solution (50/50, v/v, pH = 7.4, 20 mM). λ<sub>ex</sub> = 472 nm. Slit: 5 nm/5 nm. Note: Pd represents palladium (0).

### Selectivity

Selectivity is a very important performance for a fluorescence probe. To investigate the selectivity of Probe 1 to different metal ions, we compared the UV-vis absorption and fluorescence spectra of Probe 1 after addition of different metal ions (Na<sup>+</sup>, K<sup>+</sup>, Zn<sup>2+</sup>, Al<sup>3+</sup>, Ca<sup>2+</sup>, Fe<sup>3+</sup>, Cu<sup>2+</sup>, Mn<sup>2+</sup>, Ni<sup>2+</sup>, Cr<sup>3+</sup>, Ag<sup>+</sup>, Co<sup>2+</sup>, Pb<sup>2+</sup>, Ba<sup>2+</sup>, and Hg<sup>2+</sup>). As shown in Fig. 5, UV-vis absorption and fluorescence spectra almost have no change in the presence of Na<sup>+</sup>, K<sup>+</sup>, Zn<sup>2+</sup>, Al<sup>3+</sup>, Ca<sup>2+</sup>, Fe<sup>3+</sup>, Cu<sup>2+</sup>, Mn<sup>2+</sup>, Ni<sup>2+</sup>, Cr<sup>3+</sup>, Ag<sup>+</sup>, Co<sup>2+</sup>, Pb<sup>2+</sup>, Ba<sup>2+</sup>, and Hg<sup>2+</sup> ions except

for palladium, indicating that Probe 1 has an excellent selectivity toward palladium. Remarkably, the fluorescence intensity ratio I<sub>643</sub>/I<sub>570</sub> increases 85-fold in the presence of palladium. The corresponding color change from yellow to pink can be easily observed by naked eye (Fig. 6). Moreover, as shown in Fig. S13, Probe 1 exhibits the same sensitivity to both Pd(0) and Pd(II), which indicates that Probe 1 has generality for detecting palladium species. Fig. S14A presents the time dependent fluorescence spectrum of Probe 1 for Pd<sup>2+</sup> ions. From Fig. S14B, it can be seen that the fluorescence intensity ratio I<sub>643</sub>/I<sub>570</sub> keeps unchanged after 25 min. So, 30 min can be used as an appropriate reaction time for Pd<sup>2+</sup> detection.

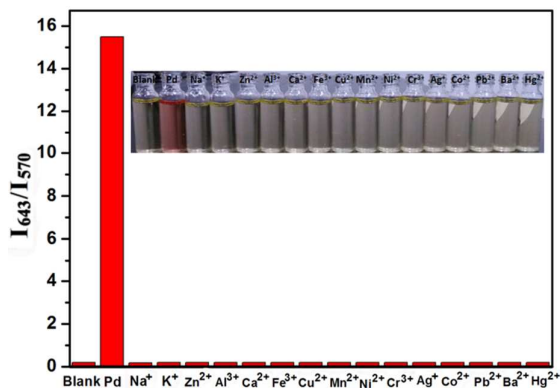


Fig. 6. Relative emission intensity ratios of Probe 1 at 643 nm and 570 nm (I<sub>643</sub>/I<sub>570</sub>) upon addition of different metal ions: Na<sup>+</sup>, K<sup>+</sup>, Zn<sup>2+</sup>, Al<sup>3+</sup>, Ca<sup>2+</sup>, Fe<sup>3+</sup>, Cu<sup>2+</sup>, Mn<sup>2+</sup>, Ni<sup>2+</sup>, Cr<sup>3+</sup>, Ag<sup>+</sup>, Co<sup>2+</sup>, Pb<sup>2+</sup>, Ba<sup>2+</sup> and Hg<sup>2+</sup> (50 μM). λ<sub>ex</sub> = 472 nm. Slit: 5 nm/5 nm. Inset: Color changes of Probe 1 after addition of different metal ions. Note: Pd represents palladium (0)

### Conclusion

We successfully synthesized a new colorimetric and ratiometric fluorescence probe (Probe 1) with red emission by using isophorone based fluorescent dye as fluorophore and allylcarbamate group as response unit. Based on the Pd<sup>0</sup>-triggered cleavage reaction under mild conditions, Probe 1 showed high response speed, selectivity, and sensitivity towards palladium species under room temperature. Moreover, Probe 1 displayed colorimetric and ratiometric responses toward palladium species. Upon addition of palladium, the absorption and emission spectra of Probe 1 exhibited obvious red-shift, corresponding to a color change from yellow to pink which can be differentiated by naked eye. In terms of palladium, the detection limit is as low as 24.2 nM and the signal-to-noise ratio in fluorescence intensity can reach 85-fold. As a ratiometric red emitting sensor, Probe 1 can be potentially used for quantitative detection of palladium in living organisms. Moreover, this work also presented a new application field for isophorone based fluorescence dyes.

### Acknowledgment

This work has been supported by the National Natural Science Foundation of China (21277046, 21173077, 21377038), the Shanghai Committee of Science and Technology (13NM1401000),

the Research Fund of Education of the People's Republic of China (JPPT-125-4-076), the National Basic Research Program of China (973 Program, 2013CB632403).

## Reference

- 1 A. L. Garner and K. Koide. *Chem. Commun.*, 2009, **1**, 86-88.
- 2 H. Chen, W. Y. Lin and L. Yuan. *Org. Biomol. Chem.*, 2013, **11**, 1938-1941.
- 3 A. L. Garner and K. Koide. *Chem. Commun.*, 2009, **1**, 83-85.
- 4 F. L. Song, A. L. Garner, K. Koide. *J. Am. Chem. Soc.*, 2007, **129**, 12354-12355.
- 5 J. Kielhorn, C. Melber, D. Keller and I. Mangelsdorf. *Int. J. Hyg. Environ. Health*, 2002, **205**, 417-432.
- 6 C. C. Wang, X. L. Zheng, R. Huang, S. Y. Yan, X. Xie, T. Tian, S. W. Huang, X. C. Weng and X. Zhou. *Asian J. Org. Chem.* 2012, **1**, 259-263.
- 7 T. Z. Liu, S. D. Lee and R. S. Bhatnagar. *Toxicology Lett.*, 1979, **4**, 469-473.
- 8 M. P. Tracey, D. Pham, K. Koide. *Chem. Soc. Rev.* 2015, DOI: 10.1039/c4cs00323c.
- 9 L. Cui, W. P. Zhu, Y. F. Xu and X. H. Qian. *Anal. Chim. Acta.*, 2013, **786**, 139-145.
- 10 C. Locatelli, D. Melucci, and G. Torsi. *Anal. Bioanal. Chem.*, 2005, **382**, 1567-1573.
- 11 K. V. Meel, A. Smekens, M. Behets, P. Kazandjian and R. Grieken. *Anal. Chem.* 2007, **79**, 6383-6389.
- 12 J. Yin, Y. H. Kwon, D. H. Kim, D. Y. Lee, G. Kim, Y. Hu, J-H Ryu and J. Yoon. *J. Am. Chem. Soc.*, 2014, **136**, 5351-5358.
- 13 S. G. Sun, B. Qiao, N. Jiang, J. T. Wang, S. Zhang and X. J. Peng. *Org. Lett.* 2014, **16**, 1132-1135.
- 14 J. Y. Wang, F. L. Song, J. Y. Wang and X. J. Peng. *Analyst*, 2013, **138**, 3667-3672.
- 15 Z. Q. Guo, S. W. Nam, S. S. Park and J. Yoon. *Chem. Sci.*, 2012, **3**, 2760-2765.
- 16 X. H. Wang, Z. Q. Guo, S. Q. Zhu, H. Tian and W. H. Zhu. *Chem. Commun.*, 2014, **50**, 13525-13528.
- 17 X. Wang, J. Sun, W. H. Zhang, X. X. Ma, J. Z. Lv and B. Tang. *Chem. Sci.*, 2013, **4**, 2551-2556.
- 18 S. Z. Pu, L. L. Ma, G. Liu, H. C. Ding and B. Chen. *Dye Pigment*, 2015, **113**, 70-77.
- 19 Y. Kubo, M. Yamamoto, M. Ikeda, M. Takeuchi, S. Shinkai, S. Yamaguchi and K. Tamao. *Angew. Chem. Int. Ed.* 2003, **42**, 2036-2040.
- 20 Z. C. Xu, X. H. Qian and J. N. Cu. *Org. Lett.*, 2005, **7**, 3029-3032.
- 21 H. L. Li, J. L. Fan, J. J. Du, K. X. Guo, S. G. Sun, X. J. Liu and X. J. Peng. *Chem. Commun.*, 2010, **46**, 1079-1081.
- 22 B. C. Zhu, C. C. Gao, Y. Z. Zhao, C. Y. Liu, Y. M. Li, Q. Wei, Z. M. Ma, B. Du and X. L. Zhang. *Chem. Commun.*, 2011, **47**, 8656-8658.
- 23 J. Y. Wang, F. L. Song, J. Y. Wang and X. J. Peng. *Analyst*, 2013, **138**, 3667-3672.
- 24 J. Jiang, H. E. Jiang, W. Liu, X. L. Tang, X. Zhou, W. S. Liu and R. L. Liu. *Org. Lett.*, 2011, **13**, 4922-4925.
- 25 A. L. Garner and K. Koide. *J. Am. Chem. Soc.*, 2008, **130**, 16472-16473.
- 26 M. E. Jun and K. H. Ahn. *Org. Lett.*, 2010, **12**, 2790-2793.
- 27 P. Hou, S. Chen, H. B. Wang, J. X. Wang, K. Voitchofsky and X. Z. Song. *Chem. Commun.*, 2014, **50**, 320-322.
- 28 X. M. Wu, X. R. Sun, Z. Q. Guo, J. B. Tang, Y. Q. Shen, T. D. James, H. Tian and W. H. Zhu. *J. Am. Chem. Soc.* 2014, **136**, 3579-3588.
- 29 B. Liu, W. H. Zhu, Q. Zhang, W. J. Wu, M. Xu, Z. J. Ning, Y. S. Xie and H. Tian. *Chem. Commun.*, 2009, **13**, 1766-1768.
- 30 Z. J. Ning, Q. Zhang, W. J. Wu, H. C. Pei, B. Liu and H. Tian. *J. Org. Chem.* 2008, **73**, 3791-3797.
- 31 O.-P. Kwon, S.-J. Kwon, M. Jazbinsek, F. D. J. Brunner, J.-I. Seo, C. Hunziker, A. Schneider, H. Yun, Y.-S. Lee and P. Günter. *Adv. Funct. Mater.* 2008, **18**, 3242-3250.
- 32 O.-P. Kwon, B. Ruiz, A. Choubey, L. Mutter, A. Schneider, M. Jazbinsek, V. Gramlich and P. Günter. *Chem. Mater.*, 2006, **18**, 4049-4054.
- 33 Z. Q. Guo, W. H. Zhu and H. Tian. *Chem. Commun.*, 2012, **48**, 6073-6084.
- 34 X. H. Wang, Z. Q. Guo, S. Q. Zhu, H. Tian and W. H. Zhu. *Chem. Commun.*, 2014, **50**, 13525-13528.
- 35 Y. Suzuki and K. Yokoyama. *J. Am. Chem. Soc.*, 2005, **127**, 17799-17802.
- 36 W. Sun, J. L. Fan, C. Hu, J. F. Cao, H. Zhang, X. Q. Xiong, J. Y. Wang, S. Cui, S. G. Sun and X. J. Peng. *Chem. Commun.*, 2013, **49**, 3890-3892.
- 37 J. V. Gompel and G. B. Schuster. *J. Org. Chem.* 1987, **52**, 1465-1468.
- 38 M. Cigán, K. Jakusová, J. Donovalová, V. Szöcs, A. Gáplovský. *RSC Adv.* 2014, **4**, 54072-54079.
- 39 C. Hu, W. Sun, J. Cao, P. Gao, J. Wang, J. Fan, F. Song, S. Sun, X. Peng. *Org. Lett.* 2013, **15** (15), 4022-4025.
- 40 W. Xuan, R. Pan, Y. Cao, K. Liu, W. Wang. *Chem. Commun.* 2012, **48**, 10669-10671.
- 41 W. Liu, J. Jiang, C. Chen, X. Tang, J. Shi, P. Zhang, K. Zhang, Z. Li, W. Dou, L. Yang, W. Liu. *Inorg. Chem.* 2014, **53** (23), 12590-12594.
- 42 L. Zhang, W-Q Meng, L. Lu, Y-S Xue, C. Li, F. Zou, Y. Liu, J. Zhao. *Scientific Reports.* 2014, **4**, 5870-5879.
- 43 M. H. Lee, J. H. Han, P-S Kwon, S. Bhuniya, J. Y. Kim, J. L. Sessler, C. Kang, J. S. Kim. *J. Am. Chem. Soc.* 2012, **134**, 1316-1322.
- 44 C. S. Lim, G. Masanta, H. J. Kim, J. H. Han, H. M. Kim, B. R. Cho. *J. Am. Chem. Soc.* 2011, **133**, 11132-11135.
- 45 A. L. Garner, F. L. Song and K. Koide. *J. Am. Chem. Soc.*, 2009, **131**, 5163-5171.